

Constraints on Scalar-Field Dark Energy from Galaxy Cluster Gas Mass Fraction versus Redshift Data

Gang Chen and Bharat Ratra

Department of Physics, Kansas State University, 116 Cardwell Hall, Manhattan, KS 66506; chengang@phys.ksu.edu, ratra@phys.ksu.edu

ABSTRACT

We use the Allen et al. (2004) *Chandra* measurements of x-ray gas mass fraction of 26 rich clusters to place constraints on the scalar-field dark energy model with inverse power law potential energy density. The constraints are consistent with, and typically more constraining than, those from other cosmological tests, and mildly favor the Einstein cosmological constant limit of the dark energy model.

Subject headings: cosmology: cosmological parameters—cosmology: observations—X-rays: galaxies: clusters

1. Introduction

All indications are that the energy budget of our universe has recently come to be dominated by some form of dark energy, resulting in an accelerating cosmological expansion. This picture is supported by a number of measurements, including: Type Ia supernova redshift-magnitude data (see, e.g., Wang & Mukherjee 2004; Nesseris & Perivolaropoulos 2004; Riess et al. 2004; Biesiada et al. 2004; Daly & Djorgovski 2004); cosmic microwave background (CMB) anisotropy data from the Wilkinson Microwave Anisotropy Probe (WMAP), with some input from other measurements (see, e.g., Bennett et al. 2003; Page et al. 2003); and, other measurements of CMB anisotropy, which indicate the universe is close to spatially flat (see, e.g., Podariu et al. 2001b; Durrer et al. 2003; Melchiorri & Ödman 2003), in combination with continuing strong evidence for low non-relativistic matter density (Chen & Ratra 2003b and references therein). For reviews see Peebles & Ratra (2003), Padmanabhan (2003), Steinhardt (2003), Carroll (2004), and Sahni (2004).

There are many proposed dark energy candidates.¹ The original example of dark energy is Einstein’s cosmological constant, Λ , which has an energy density ρ_Λ independent of time and space. The modern reincarnation of this is in the Λ CDM model (Peebles 1984), where at low redshift non-relativistic matter, dominated by the also hypothetical cold dark matter (CDM), is the other major contributor to the cosmological energy budget. More recently, dark energy models in which the dark energy density varies only slowly with time and space have attracted much attention. A simple example of such a candidate is a scalar field (ϕ) with potential energy density $V(\phi) \propto \phi^{-\alpha}$, $\alpha > 0$, at low redshift z (Peebles & Ratra 1988; Ratra & Peebles 1988); in what follows we refer to this as the ϕ CDM model. The XCDM parametrization of varying dark energy density models approximates the dark energy by a fluid with a time-independent equation of state parameter $w = p/\rho$, where p is the pressure. The XCDM parameterization is accurate in the radiation and matter dominated epochs, but much less so in the scalar field dominated epoch when w is time dependent (see, e.g., Ratra 1991). In the last two cases, consistent with observational indications, we consider only a spatially flat cosmological geometry; the Λ CDM model considered here allows space curvature to be a free parameter.

It is important to test dark energy models and constrain their parameters using as many techniques as possible. Different tests might provide different constraints on the parameters of the model, and comparison of results determined from different methods allow for consistency checks. A number of such cosmological tests have been developed. In addition to the Type Ia supernova test mentioned above², there has been discussion of the redshift-angular-size test (see, e.g., Zhu & Fujimoto 2002; Chen & Ratra 2003a; Podariu et al. 2003; Jain et al. 2003; Jackson 2003); the redshift-counts test (see, e.g., Loh & Spillar 1986; Newman & Davis 2000; Huterer & Turner 2001; Podariu & Ratra 2001); the strong gravitational lensing test (see, e.g., Fukugita et al. 1990; Turner 1990; Ratra & Quillen 1992; Waga & Frieman 2000; Chae 2003; Chae et al. 2004); and the redshift-expansion time test (see, e.g., Nolan et al. 2003; Alcaniz et al. 2003; Savage et al. 2004; Cepa 2004). Structure formation in time-variable dark energy models has also come under recent discussion (see, e.g., Mainini et al. 2003; Klypin et al. 2003; Lokas et al. 2004; Mota & van de Bruck 2004), and CMB anisotropy data is providing useful constraints (see, e.g., Mukherjee et al. 2003a, 2003b;

¹For recent discussions of dark energy models and the observational situation see Bartolo et al. (2003), Kratochvil et al. (2003), Kaplinghat & Bridle (2003), Gong (2004), Liu (2004), Gorini et al. (2004), Wetterich (2004), Matarrese et al. (2004), Bludman (2004), Feng et al. (2004) and references therein.

²The proposed SNAP/JDEM space mission to measure the redshift-magnitude relation to larger redshift should provide valuable data for constraining dark energy models (see, <http://snap.lbl.gov/> and, e.g., Podariu et al. 2001a; Weller & Albrecht 2002; Rhodes et al. 2004; Virey et al. 2004).

Caldwell & Doran 2004; Wang & Tegmark 2004; Jassal et al. 2004).

In this paper, we use the x-ray gas mass fraction of rich clusters, as a function of redshift, to constrain the three simple dark energy models mentioned above. This test was introduced by Sasaki (1996) and Pen (1997), and further developed by Allen et al. (2002, hereafter A02; also see Allen et al. 2003; Ettori et al. 2003; Allen et al. 2004, hereafter A04, and references therein).³ The basic idea is as follows. Assuming that the rich clusters are large enough to provide a fair representation of the cosmological baryon and dark matter distributions (see, e.g., White 1992; White et al. 1993; Fukugita et al. 1998), the ratio of baryonic to total mass in clusters—the cluster baryon mass fraction—should be the same as the ratio of baryonic to non-relativistic mass in the whole universe—the cosmological baryon mass fraction. The zero-redshift cluster baryon fraction test allows for a determination of the non-relativistic matter mass density parameter Ω_m from the measured cluster baryon fraction and an estimate of the baryonic mass density parameter Ω_b . If one focuses on the rich clusters (and not on those that might be in the process of collapsing), the cluster baryon mass fraction should be independent of the cluster redshift. The main contributors to the cluster baryon mass fraction are the cluster gas mass fraction and the cluster galaxy (stellar) mass fraction, with the cluster gas mass fraction dominating. The cluster gas mass fraction depends on the angular diameter distance (see, e.g., Sasaki 1996) so data on it as a function of redshift allows for another cosmological test: the correct cosmological model places the clusters at the right angular diameter distances to ensure that the gas mass fractions are independent of redshift. A02 and A04 focus on the x-ray emitting intracluster gas, and use the x-ray gas mass fraction of the total cluster mass, f_{gas} , to constrain cosmological parameters. Note that the optically luminous galaxy (stellar) mass in clusters is about $0.19h^{0.5}$ times the x-ray emitting gas mass⁴, so $\Omega_b = \Omega_m f_{\text{gas}}(1 + 0.19h^{0.5})$.

In § 2 we summarize our method of computation. Results are presented and discussed in § 3. We conclude in § 4.

³This test builds on the zero-redshift cluster baryon mass fraction test discussed by White & Frenk (1991), Fabian (1991), White (1992), and White et al. (1993).

⁴Here h is the Hubble constant in units of $100 \text{ km s}^{-1} \text{ Mpc}^{-1}$. The expression $0.19h^{0.5}$ is from A02 and is based on Fukugita et al. (1998) who use a distance-independent stellar M/L , rather than a distance-dependent dynamical M/L , so it differs from the $0.19h^{1.5}$ used by White et al. (1993).

2. Computation

We use the f_{gas} values of 26 clusters determined by A04 from *Chandra* data. These are shown in Fig. 2 of A04. The redshifts of the 26 clusters range from 0.08 to 0.89.

At low z the cosmological energy budget is dominated by the contributions from non-relativistic matter, with mass density parameter Ω_m , and dark energy, so we may ignore all other contributions. For the Λ CDM model and the XCDM parametrization, our analysis here is similar to that of A02, Allen et al. (2003), Ettori et al. (2003), Lima et al. (2003), Zhu et al. (2004), and A04, although we differ with some of these in how we use priors (discussed in § 3 below). For the ϕ CDM model we explicitly integrate the scalar field and other equations of motion (see, e.g., Peebles & Ratra 1988) to get the needed angular diameter distance.

Following A02 and A04, we fit the f_{gas} data to a model described by

$$f_{\text{gas}}^{\text{mod}}(z) = \frac{b\Omega_b}{(1 + 0.19\sqrt{h})\Omega_m} \left[\frac{h}{0.5} \frac{D_A^{\text{SCDM}}(z)}{D_A(z, \Omega_m, p)} \right]^{3/2}, \quad (1)$$

which reflects the dependence of f_{gas} on the assumed angular diameter distance (D_A) to the cluster, i.e., $f_{\text{gas}} \propto D_A^{3/2}$.⁵ Here D_A depends on the cluster redshift z , h , and the assumed cosmological model, which, for each of the three cases we consider, depends only on two parameters, Ω_m and p (where p is Ω_Λ for the Λ CDM model, α for the ϕ CDM model, and ω for the XCDM parametrization). The bias factor b accounts for gas-dynamical simulation results which indicate that the cluster baryon fraction is depressed relative to the cosmological baryon fraction (see Allen et al. 2003; A04, and references therein for detailed discussions). Following A04, uncertainties in $\Omega_b h^2$, h , and b are accounted for by using Gaussian priors. Our computations use the same Gaussian priors as A04 with $h = 0.72 \pm 0.08$, $\Omega_b h^2 = 0.0214 \pm 0.002$, and $b = 0.824 \pm 0.089$, all one standard deviation errors.⁶

⁵The A04 data used in the analysis here are determined assuming an $\Omega_m = 1$, $\Omega_\Lambda = 0$, spatially flat, standard CDM (SCDM) model with $h = 0.5$, hence the $(h/0.5)D_A^{\text{SCDM}}$ dependence of eq. (1).

⁶An analysis of all available measurements of the Hubble constant leads to a more precise estimate, $h = 0.68 \pm 0.07$ at two standard deviations (Gott et al. 2001; Chen et al. 2003), and the value quoted for $\Omega_b h^2$ in the main text, $\Omega_b h^2 = 0.0214 \pm 0.002$, is more consistent with the estimate from the WMAP CMB anisotropy data and the mean of the primordial deuterium abundance measurements, but significantly higher than estimates based on the primordial helium and lithium abundance measurements (see, e.g., Peebles & Ratra 2003; Cyburt et al. 2003; Cuoco et al. 2003; Crighton et al. 2004). Since our analysis here is preliminary, we do not carefully investigate the effect of varying the chosen parameter values, although we have repeated the analysis using the values $h = 0.68 \pm 0.04$ and $\Omega_b h^2 = 0.014 \pm 0.004$ at one standard deviation (where we have halved the above two standard deviation error bar for h and use the Peebles & Ratra 2003 summary estimate for $\Omega_b h^2$; constraints based on these numerical values are shown in the figures by using dotted lines

Including the above three parameters described by Gaussian priors, we need to compute χ^2 in a five dimensional parameter space, for the five parameters $P = (\Omega_m, p, h, \Omega_b h^2, b)$. At a given point in this parameter space the χ^2 difference between the model at this point and the data is

$$\chi^2(\Omega_m, p, h, \Omega_b h^2, b) = \sum_{i=1}^{26} \frac{[f_{\text{gas}}^{\text{mod}}(z_i, P) - f_{\text{gas},i}]^2}{\sigma_{f_{\text{gas},i}}^2} + \left[\frac{\Omega_b h^2 - 0.0214}{0.002} \right]^2 + \left[\frac{h - 0.72}{0.08} \right]^2 + \left[\frac{b - 0.824}{0.089} \right]^2 \quad (2)$$

where $f_{\text{gas}}^{\text{mod}}(z_i, P)$ is given in eq. (1), and $f_{\text{gas},i}$ and $\sigma_{f_{\text{gas},i}}$ are the measured value and error from A04 for a cluster at redshift z_i .

The probability distribution function (likelihood) of Ω_m and p is determined by marginalizing over the “nuisance” parameters

$$L(\Omega_m, p) = \int dh d(\Omega_b h^2) db e^{-\chi^2(\Omega_m, p, h, \Omega_b h^2, b)/2}, \quad (3)$$

where the integral is over a large enough range of h , $\Omega_b h^2$, and b to include almost all the probability. For each of the three cases mentioned above, we compute $L(\Omega_m, p)$ on a two-dimensional grid spanned by Ω_m and p . The 1, 2, and 3 σ confidence contours consist of points where the likelihood equals $e^{-2.30/2}$, $e^{-6.17/2}$, and $e^{-11.8/2}$ of the maximum value of the likelihood, respectively. An alternate set of confidence contours in the two-dimensional (Ω_m, p) parameter subspace may be defined by projecting the confidence contours (surfaces) from the five-dimensional (P) parameter space.⁷ We find that the projected and marginalized contours are very similar and so do not show the projected contours in our plot.

3. Results and Discussion

In the discussion below we focus mainly on the constraints that follow on using $h = 0.72 \pm 0.08$ and $\Omega_b h^2 = 0.0214 \pm 0.002$, only noting in passing the limits that follow from using $h = 0.68 \pm 0.04$ and $\Omega_b h^2 = 0.014 \pm 0.004$.

and continuous lines are used to show the constraints derived using the favored values $h = 0.72 \pm 0.08$ and $\Omega_b h^2 = 0.0214 \pm 0.002$) and find that the error bars on the estimated values of Ω_m increase by less than about 50 %, with the most favored values of Ω_m becoming smaller by about a third, compared to the results discussed below.

⁷I.e., at each point in the two-dimensional— Ω_m and p —parameter space we adjust the values of the other three parameters— h , $\Omega_b h^2$, and b —to minimize χ^2 ; this defines $\chi^2(\Omega_m, p)$ which is then used to derive the projected two-dimensional confidence contours.

The minimum value of χ^2 in the full five-dimensional parameter space is close to 24.5 for all three models considered here. At the minimum, $\Omega_m = 0.24$ in all three cases, and the other parameter p is $\Omega_\Lambda = 0.95$ in the Λ CDM model, $\omega = -1.2$ in the XCDM parametrization, and $\alpha = 0$ in the ϕ CDM model (with similar values from the two-dimensional parameter space analyses), indicating that a spatially-flat Λ CDM model is somewhat favored (in all three cases considered this model lies within one standard deviation of the most likely model).

The f_{gas} constraints we derive on the Λ CDM model (Fig. 1, continuous lines) and on the XCDM parameters (Fig. 2, continuous lines) are quite similar to those in Figs. 4 and 10 of A04. As noted in A04, for Λ CDM these f_{gas} constraints are consistent with those from CMB anisotropy data and the brightness of distant Type Ia supernovae provided $\Omega_m \sim 0.3$ and $\Omega_\Lambda \sim 0.7$. Using only the 9 clusters f_{gas} data of Allen et al. (2003), our XCDM parametrization confidence contours are about twice as wide as those in Fig. 3 of Lima et al. (2003) and Fig. 3 of Zhu et al. (2004). This is because Lima et al. (2003) and Zhu et al. (2004) effectively use a Dirac-delta-like prior, akin to fixing h , $\Omega_b h^2$, and b at their favored central values and to setting the last three terms in eq. (2) to zero.

Figure 3 (continuous lines) shows the f_{gas} constraints on the ϕ CDM model. These contours are tighter than those derived from the (older) Type Ia supernova redshift-magnitude data (Podariu & Ratra 2000; Waga & Frieman 2000), redshift-angular size data (Chen & Ratra 2003a; Podariu et al. 2003), or gravitational lensing statistics (Chae et al. 2004). The ϕ CDM model is consistent with all of these tests when $0.15 \lesssim \Omega_m \lesssim 0.35$ and $\alpha \lesssim 2$ (at two standard deviations; the numerical values are modified if we instead use the priors of footnote 6, with a larger range of parameter space being acceptable). This range of parameters is also consistent with large scale structure and large angle CMB anisotropy data when $\Omega_b h^2$ is near the lower end of the allowed range (Mukherjee et al. 2003b).

In all three figures we also show the constraints (dotted lines) that result from using $h = 0.68 \pm 0.04$ and $\Omega_b h^2 = 0.014 \pm 0.004$. Comparing these contours to those discussed above (continuous lines) gives an indication of the size of the systematic effects on parameter determination.

4. Conclusion

We use recent x-ray cluster gas mass fraction data from the *Chandra* observatory to constrain cosmological parameters. These constraints are consistent with those derived from other cosmological tests for a range of parameter values in each of the three cases we consider, but mildly favor the spatially-flat Λ CDM model. The f_{gas} data is efficacious at constraining

dark energy, and also provides a relatively tight and approximately model-independent constraint on Ω_m , $0.15 \lesssim \Omega_m \lesssim 0.35$ at two standard deviations, which is in good accord with other recent estimates (Chen & Ratra 2003b; Bennett et al. 2003). Future f_{gas} data should provide an even tighter constraint and is eagerly anticipated.

We are indebted to S. Allen for providing the cluster gas mass fraction data and helpful discussions. We also acknowledge helpful discussions with J. Alcaniz, J. Peebles, and Z. Zhu, and support from NSF CAREER grant AST-9875031 and DOE EPSCoR grant DE-FG02-00ER45824. We thank the referee for useful advice.

REFERENCES

- Alcaniz, J. S., Lima, J. A. S., & Cunha, J. V. 2003, MNRAS, 340, L39
- Allen, S. W., Schmidt, R. W., Ebeling, H., Fabian, A. C., & van Speybroeck, L. 2004, MNRAS, in press, astro-ph/0405340 (A04)
- Allen, S. W., Schmidt, R. W., & Fabian, A. C. 2002, MNRAS, 334, L11 (A02)
- Allen, S. W., Schmidt, R. W., Fabian, A. C., & Ebeling, H. 2003, MNRAS, 342, 287
- Bartolo, N., Corasaniti, P.-S., Liddle, A. R., & Malquarti, M. 2003, astro-ph/0311503
- Bennett, C. L., et al. 2003, ApJS, 148, 1
- Biesiada, M., Godłowski, W., & Szydlowski, M. 2004, astro-ph/0403305
- Bludman, S. 2004, astro-ph/0403526
- Caldwell, R. R., & Doran, M. 2004, Phys. Rev. D, 69, 103517
- Carroll, S. M. 2004, in Measuring and Modeling the Universe, ed. W. L. Freedman (Cambridge: Cambridge University Press), 235
- Cepa, J. 2004, astro-ph/0403616
- Chae, K.-H. 2003, MNRAS, 346, 746
- Chae, K.-H., Chen, G., Ratra, B., & Lee, D.-W. 2004, ApJ, 607, L71
- Chen, G., Gott, J. R., & Ratra, B. 2003, PASP, 115, 1269
- Chen, G., & Ratra, B. 2003a, ApJ, 582, 586

- Chen, G., & Ratra, B. 2003b, *PASP*, 115, 1143
- Crighton, N. H. M., Webb, J. K., Ortiz-Gil, A., & Fernández-Soto, A. 2004, *astro-ph/0403512*
- Cuoco, A., Iocco, F., Mangano, G., Miele, G., Pisanti, O., & Serpico, P. D. 2003, *astro-ph/0307213*
- Cyburt, R. H., Fields, B. D., & Olive, K. A. 2003, *Phys. Lett. B*, 567, 227
- Daly, R. A., & Djorgovski, S. G. 2004, *ApJ*, in press, *astro-ph/0403664*
- Durrer, R., Novosyadlyj, B., & Apunevych, S. 2003, *ApJ*, 583, 33
- Ettori, S., Tozzi, P., & Rosati, P. 2003, *A&A*, 398, 879
- Fabian, A. C. 1991, *MNRAS*, 253, 29P
- Feng, B., Wang, X., & Zhang, X. 2004, *astro-ph/0404224*
- Fukugita, M., Futamase, T., & Kasai, M. 1990, *MNRAS*, 246, 24P
- Fukugita, M., Hogan, C. J., & Peebles, P. J. E. 1998, *ApJ*, 503, 518
- Gong, Y. 2004, *astro-ph/0401207*
- Gorini, V., Kamenshchik, A., Moschella, U., & Pasquier, V. 2004, *gr-qc/0403062*
- Gott, J. R., Vogeley, M. S., Podariu, S., & Ratra, B. 2001, *ApJ*, 549, 1
- Huterer, D., & Turner, M. S. 2001, *Phys. Rev. D*, 64, 123527
- Jackson, J. C. 2003, *astro-ph/0309390*
- Jain, D., Dev, A., & Alcaniz, J. S. 2003, *Class. Quant. Grav.*, 20, 4163
- Jassal, H. K., Bagla, J. S., & Padmanabhan, T. 2004, *astro-ph/0404378*
- Kaplinghat, M., & Bridle, S. 2003, *astro-ph/0312430*
- Klypin, A., Macciò, A. V., Mainini, R., & Bonometto, S. A. 2003, *ApJ*, 599, 31
- Kratochvil, J., Linde, A., Linder, E. V., & Shmakova, M. 2003, *astro-ph/0312183*
- Lima, J. A. S., Cunha, J. V., & Alcaniz, J. S. 2003, *Phys. Rev. D*, 68, 023510
- Liu, J. 2004, *Phys. Rev. D*, 69, 083504

- Loh, E. D., & Spillar, E. J. 1986, ApJ, 307, L1
- Lokas, E. L., Bode, P., & Hoffman, Y. 2004, MNRAS, 349, 595
- Mainini, R., Macciò, A. V., Bonometto, S. A., & Klypin, A., 2003, ApJ, 599, 24
- Matarrese, S., Baccigalupi, C., & Perrotta, F. 2004, astro-ph/0403480
- Melchiorri, A., & Ödman, C. J. 2003, Phys. Rev. D, 67, 081302
- Mota, D. F., & van de Bruck, C. 2004, A&A, 421, 71
- Mukherjee, P., Banday, A. J., Riazuelo, A., Górski, K. M., & Ratra, B. 2003b, ApJ, 598, 767
- Mukherjee, P., Ganga, K., Ratra, B., Rocha, G., Souradeep, T., Sugiyama, N., & Górski, K. M. 2003a, Intl. J. Mod. Phys. A, 18, 4933
- Nesseris, S., & Perivolaropoulos, L. 2004, astro-ph/0401556
- Newman, J. A., & Davis, M. 2000, ApJ, 534, L11
- Nolan, L. A., Dunlop, J. S., Jimenez, R., & Heavens, A. F. 2003, MNRAS, 341, 464
- Padmanabhan, T. 2003, Phys. Repts., 380, 235
- Page, L., et al. 2003, ApJS, 148, 233
- Peebles, P. J. E. 1984, ApJ, 284, 439
- Peebles, P. J. E., & Ratra, B. 1988, ApJ, 325, L17
- Peebles, P. J. E., & Ratra, B. 2003, Rev. Mod. Phys., 75, 559
- Pen, U. 1997, New Astro., 2, 309
- Podariu, S., Daly, R. A., Mory, M. P., & Ratra, B. 2003, ApJ, 584, 577
- Podariu, S., Nugent, P., & Ratra, B. 2001a, ApJ, 553, 39
- Podariu, S., & Ratra, B. 2000, ApJ, 532, 109
- Podariu, S., & Ratra, B. 2001, ApJ, 563, 28
- Podariu, S., Souradeep, T., Gott, J. R., Ratra, B., & Vogeley, M. S. 2001b, ApJ, 559, 9
- Ratra, B. 1991, Phys. Rev. D, 43, 3802

- Ratra, B., & Peebles, P. J. E. 1988, *Phys. Rev. D*, 37, 3406
- Ratra, B., & Quillen, A. 1992, *MNRAS*, 259, 738
- Rhodes, J., et al. 2004, *Astropart. Phys.*, 20, 377
- Riess, A. G., et al. 2004, *ApJ*, 607, 665
- Sahni, V. 2004, astro-ph/0403324
- Sasaki, S. 1996, *PASJ*, 48, L119
- Savage, C., Sugiyama, N., & Freese, K. 2004, astro-ph/0403196
- Steinhardt, P. J. 2003, *Phil. Trans. Roy. Soc. Lond. A*, 361, 2497
- Turner, E. L. 1990, *ApJ*, 365, L43
- Virey, J.-M., Taxil, P., Tilquin, A., Ealet, A., Fouchez, D., & Tao, C. 2004, astro-ph/0403285
- Waga, I., & Frieman, J. A. 2000, *Phys. Rev. D*, 62, 043521
- Wang, Y., & Mukherjee, P. 2004, *ApJ*, 606, 654
- Wang, Y., & Tegmark, M. 2004, *Phys. Rev. Lett.*, 92, 241302
- Weller, J., & Albrecht, A. 2002, *Phys. Rev. D*, 65, 103512
- Wetterich, C. 2004, astro-ph/0403289
- White, S. D. M. 1992, in *Clusters and Superclusters of Galaxies*, ed. A. C. Fabian (Dordrecht: Kluwer), 17
- White, S. D. M., & Frenk, C. S. 1991, *ApJ*, 379, 52
- White, S. D. M., Navarro, J. F., Evrard, A. E., & Frenk, C. S. 1993, *Nature*, 366, 429
- Zhu, Z.-H., & Fujimoto, M.-K. 2002, *ApJ*, 581, 1
- Zhu, Z.-H., Fujimoto, M.-K., & He, X.-T. 2004, *A&A*, 417, 833

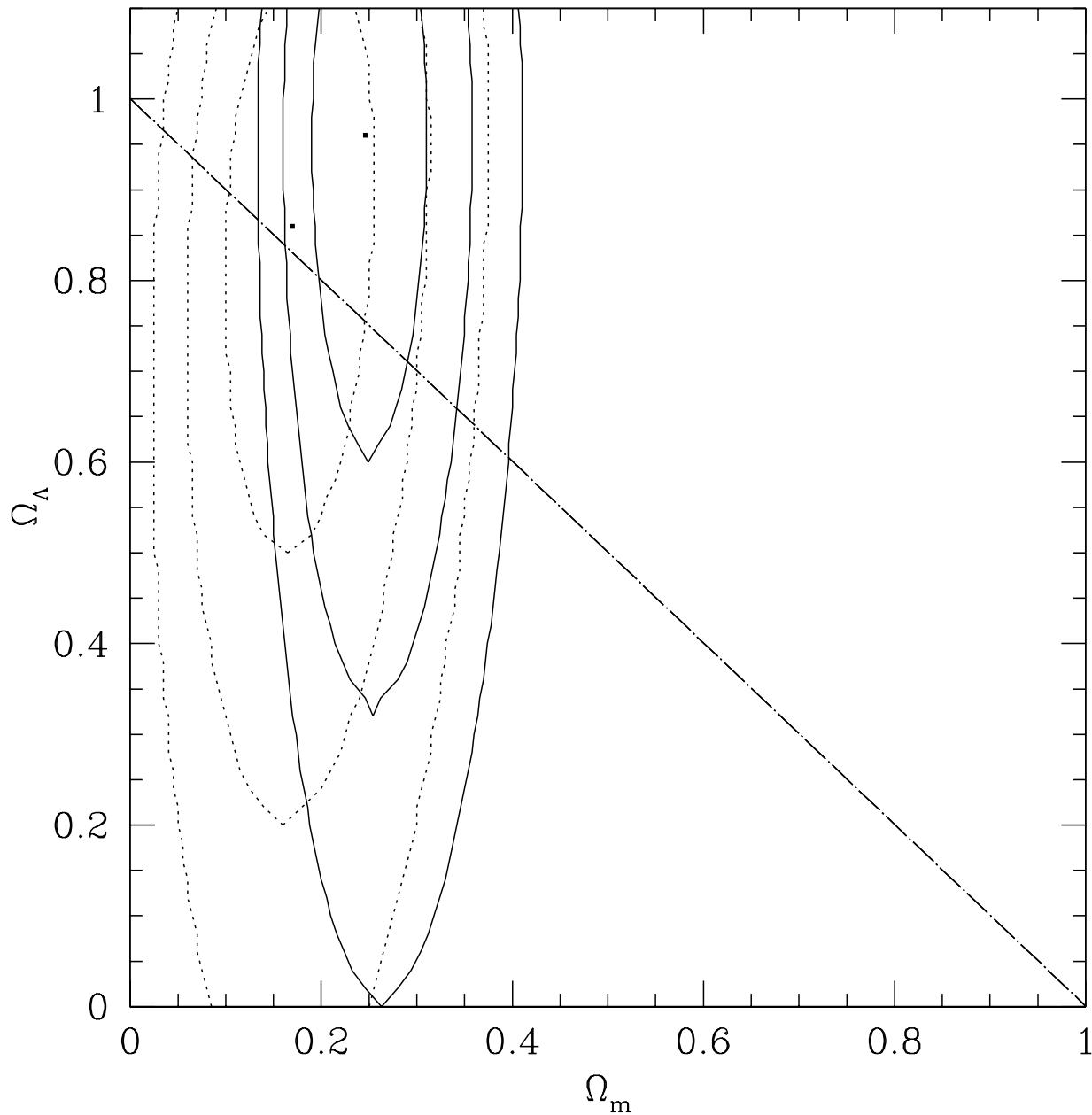


Fig. 1.— Contours of 1, 2, and 3 σ confidence (from inside to outside) for the Λ CDM model. Continuous lines are computed using $h = 0.72 \pm 0.08$ and $\Omega_b h^2 = 0.0214 \pm 0.002$ while dotted lines are based on $h = 0.68 \pm 0.04$ and $\Omega_b h^2 = 0.014 \pm 0.004$. The two dots denote where the likelihood is maximum. The diagonal dot-dashed line demarcates spatially-flat models.

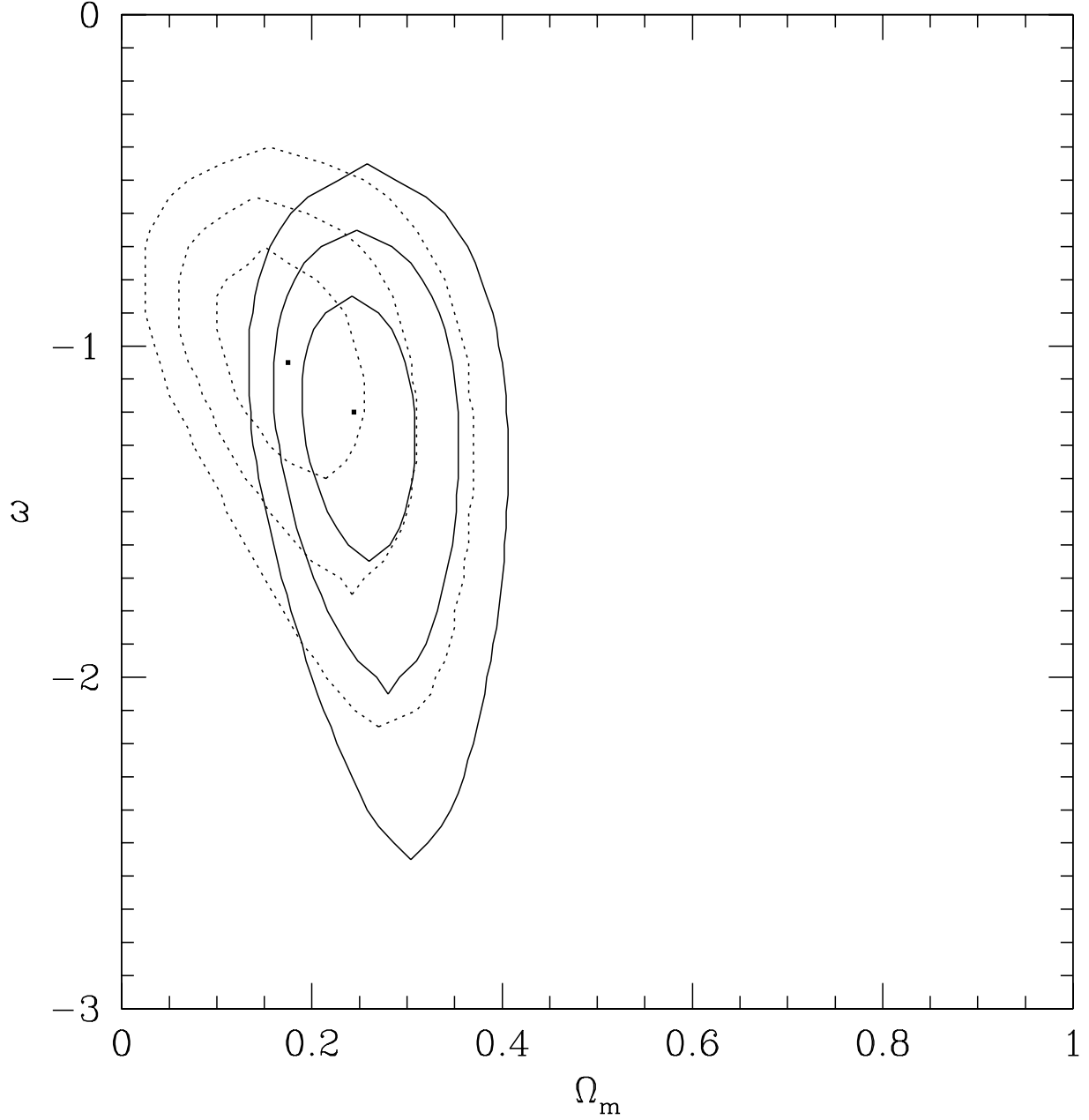


Fig. 2.— Contours of 1, 2, and 3 σ confidence (from inside to outside) for the XCDM parameters. Continuous lines are computed using $h = 0.72 \pm 0.08$ and $\Omega_b h^2 = 0.0214 \pm 0.002$ while dotted lines are based on $h = 0.68 \pm 0.04$ and $\Omega_b h^2 = 0.014 \pm 0.004$. The two dots denote where the likelihood is maximum.

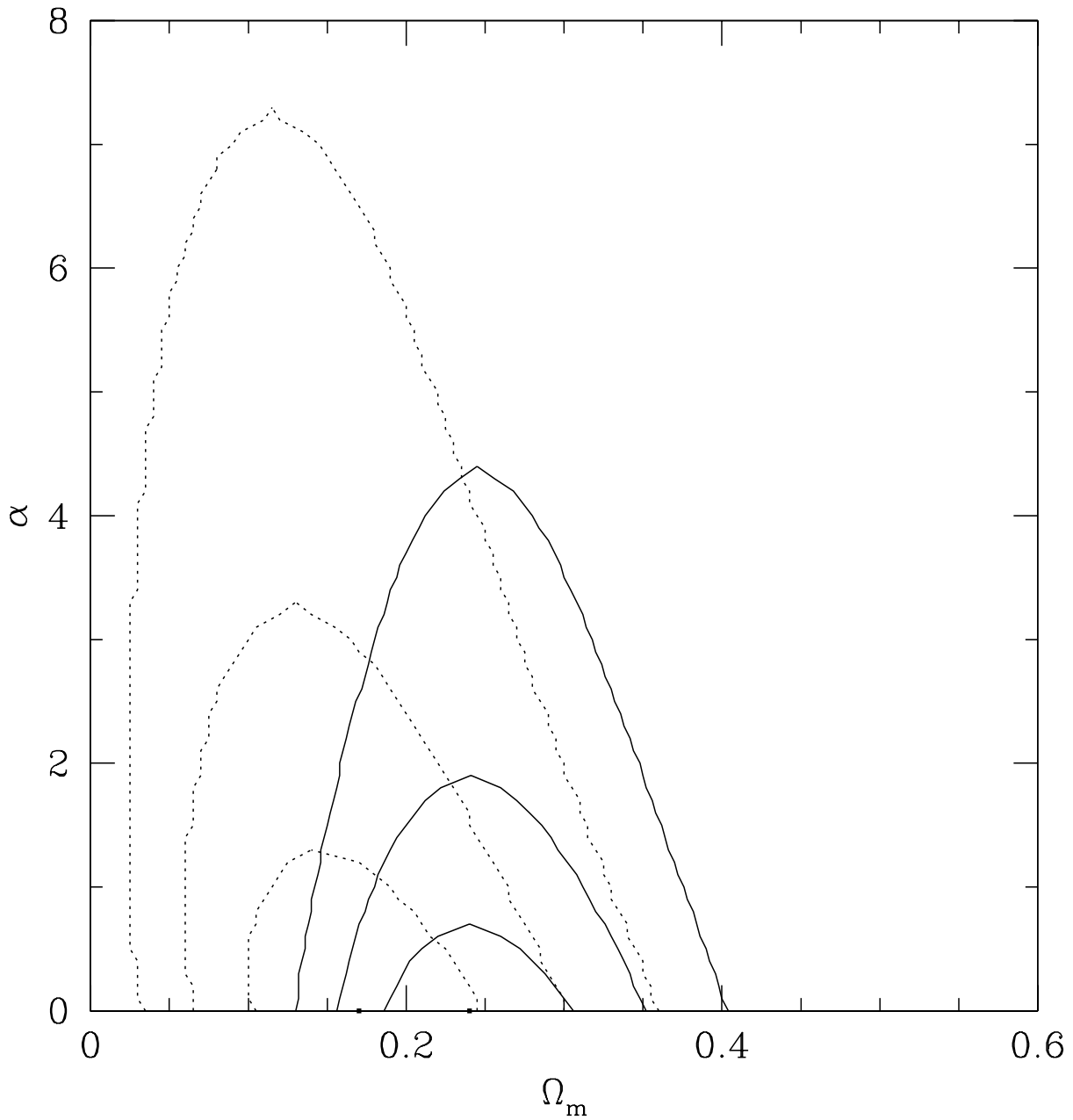


Fig. 3.— Contours of 1, 2, and 3 σ confidence (from inside to outside) for the spatially-flat ϕ CDM model with inverse power law scalar field potential energy density $V(\phi) \propto \phi^{-\alpha}$ and non-relativistic CDM. Continuous lines are computed using $h = 0.72 \pm 0.08$ and $\Omega_b h^2 = 0.0214 \pm 0.002$ while dotted lines are based on $h = 0.68 \pm 0.04$ and $\Omega_b h^2 = 0.014 \pm 0.004$. The two dots denote where the likelihood is maximum.